

# Peak effect, vortex-lattice melting-line and order–disorder transition in conventional and high- $T_c$ superconductors

Grigorii P. Mikitik

*B. Verkin Institute for Low Temperature Physics & Engineering, National Ukrainian Academy of Sciences, Kharkov 61103, Ukraine*

Ernst Helmut Brandt

*Max-Planck-Institut für Metallforschung, D-70506 Stuttgart, Germany*  
(November 12, 2018)

We investigate the order–disorder transition line from a Bragg glass to an amorphous vortex glass in the  $H - T$  phase diagram of three-dimensional type-II superconductors taking into account both pinning-caused and thermal fluctuations of the vortex lattice. Our approach is based on the Lindemann criterion and on results of the collective pinning theory and generalizes previous work of other authors. It is shown that the shapes of the order–disorder transition line and the vortex lattice melting curve are determined only by the Ginzburg number, which characterizes thermal fluctuations, and by a parameter which describes the strength of the quenched disorder in the flux-line lattice. In the framework of this unified approach we obtain the  $H - T$  phase diagrams for both conventional and high- $T_c$  superconductors. Several well-known experimental results concerning the fishtail effect and the phase diagram of high- $T_c$  superconductors are naturally explained by assuming that a peak effect in the critical current density versus  $H$  signalizes the order–disorder transition line in superconductors with point defects.

PACS numbers: 74.60.Ge, 74.72.Bk

## I. INTRODUCTION

In type-II superconductors one often observes<sup>1–16</sup> a peak effect (or fishtail effect) in the critical current density measured as a function of the applied magnetic field  $H$  at a fixed temperature  $T$  or as a function of  $T$  at fixed  $H$ . In conventional low- $T_c$  materials this peak effect mainly occurs at magnetic fields  $H$  near the upper critical field  $H_{c2}(T)$ .<sup>1–5</sup> In the high- $T_c$  YBaCuO crystals, the line of the maximum critical current density,  $H_p(T)$ , frequently lies essentially below the irreversibility line in the  $H - T$  plane,<sup>6–9</sup> and in sufficiently perfect crystals it exhibits *nonmonotonic* behavior with temperature.<sup>10–16</sup> In these perfect crystals the line of maximum current density approaches the flux-line melting line,  $H_m(T)$ , approximately at the so-called upper critical point<sup>17</sup> at which the melting line terminates. When the oxygen deficiency  $\delta$  in YBa<sub>2</sub>Cu<sub>3</sub>O<sub>7- $\delta$</sub>  increases or the crystal becomes less perfect, the end point tends to the superconducting transition temperature  $T_c$  at zero magnetic field, while  $H_p(T)$  becomes a monotonically decreasing function.<sup>11,16</sup> It is also important to note that at a fixed oxygen concentration the fishtail effect can disappear in pure YBaCuO crystals if the distribution of the oxygen vacancies over the sample becomes uniform.<sup>18</sup>

At present the origin of the peak effect in low- $T_c$  and high- $T_c$  superconductors is commonly associated with the proliferation of dislocations in the flux-line lattice.<sup>1–5,10–16</sup> At this first order phase transition<sup>3,19–22</sup> induced by quenched disorder in the vortex system, a transformation of a quasicrystalline Bragg glass<sup>23</sup> into a disordered amorphous vortex phase occurs. Although dif-

ferent criteria<sup>3,12–14</sup> are used for determining the exact position of this transition on the peak-shaped dependence of the critical current density on  $H$ , they all lead to qualitatively similar  $H - T$  phase diagrams, and, for definiteness only, we shall imply below that the phase transition corresponds to the line of the maximum critical current density,  $H_p(T)$ .

A description of this order–disorder phase transition in high- $T_c$  superconductors was proposed in Refs. 24–26 using the Lindemann criterion. It was implied in these papers that the nature of the order–disorder phase transition is different from the vortex lattice melting transition, but at the critical point both phase transition lines merge. Recently it was refined<sup>22</sup> that the upper critical point does not generally coincide with the point where the order–disorder line reaches the melting curve, and thus the melting line has a portion beyond the intersection point. However, the following should be noted: The results of Refs. 24–26 for the disorder–induced transition were obtained in the regime of single vortex pinning<sup>27</sup> when the Larkin pinning length  $L_c$  is less than  $L_0 = \epsilon a$  where  $a = (\Phi_0/H)^{1/2}$  is the spacing between flux lines,  $\Phi_0$  is the flux quantum, and  $\epsilon = \lambda_{ab}/\lambda_c \leq 1$  is the anisotropy of the superconductor ( $\lambda_{ab}$ ,  $\lambda_c$  are the London penetration depths in the  $ab$  plane and along the  $c$  axis, respectively). When  $T$  increases, the length  $L_c$  should exceed  $\epsilon a$  at some temperature which lies on the boundary of the single vortex pinning regime. At higher temperatures the disorder was completely neglected in Refs. 24–26, and only the melting line of the ideal lattice was derived. Thus, the behavior of the order–disorder line was not actually investigated in the high tempera-

ture region, and its connection with the melting line was not established. Besides this, it has remained unclear why the proliferation of dislocations in the vortex lattice of high- $T_c$  and low- $T_c$  superconductors leads to different phase diagrams.

In the present paper we consider the order-disorder transition line in the high temperature region and *obtain* the point where the vortex lattice melting and the order-disorder transition lines merge. It turns out that for a given model of the vortex pinning, the resulting  $H - T$  phase diagram is determined only by the Ginzburg number  $Gi$ , which characterizes the thermal fluctuations, and by a parameter<sup>27</sup>  $j_c(0)/j_0(0)$  that describes the strength of the quenched disorder in the flux-line lattice at  $T = 0$  ( $j_0$  is the depairing current density and  $j_c$  is the critical current density in the single vortex pinning regime; both are in the  $ab$  plane). For different values of these parameters, phase diagrams are obtained which are similar to those observed in experiments for low- $T_c$  and high- $T_c$  superconductors. Thus, the results of this paper provide a unified approach for analyzing  $H - T$  phase diagrams of various superconductors.

In this paper we consider only magnetic fields exceeding considerably the lower critical field  $H_{c1}$  and thus disregard the reentrant behavior of the melting transition and do not distinguish between the magnetic field  $H$  and the magnetic induction  $B$ . Besides this, we deal only with anisotropic three-dimensional superconductors, neglecting completely the decoupling of the superconducting layers. We also assume that  $\mathbf{H}$  is directed along the  $c$  axis. This assumption simplifies the analysis of the problem, though our final Eqs. (19) to (25) are valid for any direction of the magnetic field.

## II. LINDEMANN CRITERION

We begin with simple estimates which show that the Lindemann criterion does define the condition for proliferation of dislocations in the flux-line lattice at the order-disorder transition. Consider a dislocation network in the lattice. Let a unit cell of this network have the dimensions  $R_d$  and  $L_d$  in the transverse and longitudinal directions to  $\mathbf{H}$ , respectively. A comparison of tilt and shear elastic energies yields that  $L_d/R_d \sim [c_{44}(1/R_d, 1/L_d)/c_{66}]^{1/2} > 1$  where  $c_{66}$  and  $c_{44}(k_\perp, k_\parallel)$  are the shear and nonlocal tilt moduli of the flux-line lattice.<sup>28</sup> The energy cost for the creation of a dislocation cell is of the order of

$$E_d \sim \varepsilon_0 L_d$$

where  $\varepsilon_0 = (\Phi_0/4\pi\lambda_{ab})^2$  and  $\lambda_{ab}$  is the London penetration depth for currents in the  $ab$  plane. On the other hand, the elastic energy in the volume  $R_d^2 L_d$  is estimated as

$$E_{el} \sim c_{66} L_d u^2(R_d, L_d)$$

where  $u^2(R, L)$  is the correlation function determining the relative displacement of points in the lattice with quenched disorder,

$$u(R, L) \equiv \langle [\mathbf{u}(R, L) - \mathbf{u}(0, 0)]^2 \rangle^{1/2}.$$

Here  $\mathbf{u}$  is the transverse displacement of a flux line,  $\langle \dots \rangle$  means averaging over both thermal and quenched disorder, the first coordinate  $R$  in  $\mathbf{u}(R, L)$  indicates the position of the flux line in the plane normal to the applied magnetic field, while the second coordinate  $L$  defines the position of a point on the flux line. Comparing  $E_d$  and  $E_{el}$  with account of  $c_{66} \sim \varepsilon_0/a^2$ , one arrives at the conclusion that a dislocation network can exist in the lattice if  $u(R_d, L_d) \geq a$ . In other words,  $R_d$  should be greater than the so called positional correlation length  $R_a$  within which typical relative vortex displacements are of the order of the lattice spacing  $a$ . However, this is only a necessary but not sufficient condition for the existence of dislocations. Displacements generated by the dislocations facilitate a better adjustment of the vortex lattice to the quenched disorder. The relative deformation of the lattice produced by the dislocations is of the order of  $a/R_d$ . Therefore, the smaller  $R_d$  is the greater is the gain  $\delta E_{pin}$  in pinning energy  $E_{pin}$ . Thus, the network first appears at the smallest possible  $R_d$ , and we arrive at the result  $R_d \sim R_a$  (and  $L_d \sim L_a$ ) obtained in Ref. 22. The relative magnitude of the gain,  $\delta E_{pin}/E_{pin}$  is determined by the ratio  $a/R_a$ . Hence, for this magnitude to become of the order of unity,  $R_a/a$  should decrease to a certain constant  $C$ ,

$$\frac{R_a}{a} = C.$$

This criterion for the appearance of dislocations in the flux-line lattice was obtained in Refs. 22,29 (see also Ref. 1), and is equivalent<sup>30</sup> to the condition<sup>25</sup>:

$$u^2(a, 0) = c_L^2 a^2, \quad (1)$$

where  $c_L$  is the phenomenological Lindemann constant. This immediately follows from the fact that the ratio of  $u(R_a, 0)$  to  $u(a, 0)$  [i.e.,  $a/u(a, 0)$ ] is a function of  $R_a/a$ . Finally, since  $u(a, 0) = u(0, L_0)$  at  $L_0 = \epsilon a$ ,<sup>27</sup> one more form of the Lindemann criterion exists:

$$u^2(0, L_0) = c_L^2 a^2. \quad (2)$$

It is just this form that was used in Refs. 24,26.

Strictly speaking, the values of the constants  $C$  and  $c_L$  may depend on whether the order-disorder transition occurs in the single vortex pinning region or in the region of bundle pinning. However, to understand the essence of the matter, we shall use the simplest approximation:  $c_L$  will be considered as the same constant for the various regimes of pinning.

### III. THE ORDER-DISORDER LINE. SIMPLIFIED APPROACH

As well-known,<sup>27,31</sup> thermal fluctuations of the flux-line lattice lead to a smoothing of the pinning potential and thereby affect the pinning. This thermal depinning is especially important for high- $T_c$  superconductors. However, to elucidate possible types of the order-disorder transition line, in this section we completely disregard the thermal fluctuations. The influence of the thermal depinning on the order-disorder line will be analyzed in Sec. IV.

#### A. Region of single vortex pinning

As has been mentioned above, the order-disorder line  $H_{dis}(T)$  was studied<sup>24-26</sup> inside the single-vortex pinning regime where the Larkin pinning length  $L_c$  is less than  $L_0 = \epsilon a$ . Since  $L_0 > L_c$ , formulas of the random manifold regime<sup>27</sup> for a single vortex are applicable to calculate the displacement correlation  $u(0, L_0)$ ,

$$u(0, L_0) \approx \xi (L_0/L_c)^\zeta, \quad (3)$$

where  $\xi$  is the coherence length in the  $ab$  plane and  $\zeta$  is the roughness exponent for a flux line. In Ref. 26 the value  $\zeta \approx 3/5$  was used, while  $\zeta \approx 5/8$  in Ref. 24. Inserting Eq. (3) into Eq. (2), we obtain after simple manipulations:

$$H_{dis} = \frac{\Phi_0 c_L^2}{\xi^2} \left( \frac{c_L L_c}{\epsilon \xi} \right)^\alpha, \quad (4)$$

where  $\alpha = 2\zeta/(1-\zeta) \approx 3$ . Eq. (4) coincides with the appropriate formulas of Refs. 24-26. For Eq. (4) to be self-consistent, it is necessary to verify that  $L_0 > L_c$  at  $H = H_{dis}$  or in other words  $H_{dis} < H_{sv}$  where  $H_{sv} = \Phi_0 \epsilon^2 / L_c^2$  is the boundary of the single vortex pinning regime.<sup>27</sup> This condition yields:

$$\frac{\epsilon \xi}{L_c} > c_L. \quad (5)$$

If the inequality (5) is not fulfilled, Eq. (4) is not valid to describe  $H_{dis}$ .

The parameter  $\epsilon \xi / L_c$  generally depends on the temperature  $T$ . For example, according to simple estimates given in Appendix A, Eqs. (A3), (A7), it decreases with  $T$  and reaches zero at  $T = T_c$ . Moreover, its decrease becomes especially pronounced if the thermal depinning is taken into account. [In this case the single vortex collective pinning length  $L_c$  increases sharply<sup>27</sup> when  $T$  exceeds the characteristic pinning energy  $T_{dp}^s(T)$ , see Appendix A.] Thus, even if  $\epsilon \xi(0)/c_L L_c(0) > 1$ , the order-disorder line  $H_{dis}(T)$  reaches the boundary of the single vortex pinning regime,  $H_{sv}(T)$ , at some temperature  $T_1$  defined by the condition

$$\frac{\epsilon \xi(T_1)}{L_c(T_1)} = c_L, \quad (6)$$

and at  $T > T_1$ , Eq. (4) fails.

It is worth noting that the parameter  $\epsilon \xi / L_c$  appearing in Eqs. (4) - (6) and formulas given below characterizes the strength of the disorder in the flux-line lattice<sup>27</sup> and is expressed through the critical current density  $j_c$  in the single vortex pinning regime,

$$\frac{\epsilon \xi}{L_c} = \left( \frac{j_c}{j_0} \right)^{1/2}, \quad (7)$$

where  $j_0$  is the depairing current density.

#### B. High temperature region

At  $T > T_1$  the order-disorder transition line lies above  $H_{sv}(T)$ . In this region of the  $H - T$  plane small-bundle and large-bundle regimes of pinning occur.<sup>27</sup> Hence the transverse collective pinning length  $R_c$  exceeds  $a$ , and to find  $u(a, 0)$ , the results<sup>27,32,33</sup> may be used, which were obtained within the framework of the perturbative approach of Larkin and Ovchinnikov.<sup>32</sup> We have:

$$u^2(a, 0) \approx \xi^2 (L_0/L_c)^3 \left( \frac{1 - h_{sv}}{1 - h} \right)^{3/2}, \quad (8)$$

where  $L_0 = \epsilon a$ ,  $h \equiv H/H_{c2}$ ,  $h_{sv} \equiv H_{sv}/H_{c2}$ , the upper critical field  $H_{c2} = \Phi_0/2\pi\xi^2$ , and  $L_c$  is the *single vortex* collective pinning length. Note that Eq. (8) differs from formula (4.17) of Ref. 27 by the last factor containing  $h$  and  $h_{sv}$ . This factor takes into account the possibility that  $1 - h$  is small; in Ref. 27 the correlation function  $u^2(R, L)$  is given without taking account of this possibility. The origin of this factor is the following. The quantity  $u^2$  is proportional to  $n f_{pin}^2 \lambda_{ab} / H_{c66}^{3/2}$ . When  $h \rightarrow 1$ , one has  $\lambda_{ab} \propto (1 - h)^{-1/2}$ ,  $c_{66} \propto (1 - h)^2$  (see Ref. 28,34), while  $f_{pin}^2 \propto \epsilon_0^2 \propto (1 - h)^2$  (see Ref. 32 and also Appendix A). The combination of these factors gives Eq. (8), in which the additional constant factor  $(1 - h_{sv})^{3/2}$  has been introduced to provide a smooth crossover of this expression to the appropriate formula for the single vortex pinning regime at  $h = h_{sv}$ .

Inserting formula (8) into Eq. (1), we obtain an equation for  $h_{dis} = H_{dis}/H_{c2}$ ,

$$h_{dis}(1 - h_{dis})^3 = 2\pi c_L^2 \left( \frac{\epsilon \xi}{c_L L_c} \right)^6 (1 - h_{sv})^3, \quad (9)$$

where  $h_{sv} = H_{sv}/H_{c2} = 2\pi(\epsilon \xi / L_c)^2$  and the right hand side depends only on the temperature. Note that at  $T = T_1$ , when  $\epsilon \xi / L_c = c_L$ , one has  $h_{dis}(T_1) = 2\pi c_L^2 = h_{sv}(T_1)$ , in agreement with Eq. (4). A simple analysis shows that  $2\pi c_L^2$  should be greater than 0.25 but less than 1 (i.e.,  $0.2 \leq c_L \leq 0.4$ ) for Eq. (9) to have a solution at

$T \geq T_1$ . If  $c_L < 0.2$ , the order-disorder line terminates at  $T = T_1$ , which is impossible.<sup>35</sup> On the other hand, if  $c_L > 0.4$ , one finds from Eq. (9) that  $h_{dis} > 1 - h_{sv}$ , i.e., the root of the equation lies in the upper region of single vortex pinning<sup>36</sup> where Eq. (9) is not valid. For this reason, in the following we assume the conditions  $0.2 \leq c_L \leq 0.4$  to be fulfilled and, for definiteness, take  $c_L = 0.25$  in the subsequent calculations.

### C. Types of phase diagrams

We begin the analysis of phase diagrams with the case

$$D > c_L$$

where  $D \equiv \epsilon\xi(0)/L_c(0)$  is the value of the parameter  $\epsilon\xi/L_c$  at  $T = 0$ . Figure 1 shows the line  $H_{dis}(T)$  calculated by solving Eq. (9) (for  $H_{dis} > H_{sv}$ ) and Eq. (4) (for  $H_{dis} < H_{sv}$ ). In the construction of this figure, as well as in all examples below, we use  $H_{c2}(T) = H_{c2}(0)[1 - (T/T_c)^2]$  and  $\alpha = 3$  (i.e.,  $\zeta = 3/5$ ). Besides this, taking into account the formula (A13) of Appendix A, we employ the following simple approximation for the parameter  $\epsilon\xi/L_c$ :

$$\frac{\epsilon\xi(T)}{L_c(T)} \equiv Dg_0(t) \quad (10)$$

with

$$g_0(t) = (1 - t^2)^{1/2}, \quad (11)$$

where  $t \equiv T/T_c$ . The increase of  $H_{dis}$  and its subsequent maximum are seen in the vicinity of  $T_1$ . As to  $h_{dis}$ , this normalized quantity increases monotonically above  $T_1$ . When  $1 - h_{dis} \ll 1$ , an approximate solution of Eq. (9) is:

$$\frac{H_{dis}(T)}{H_{c2}(T)} \approx 1 - \left(\frac{2\pi}{c_L^4}\right)^{1/3} \left(\frac{\epsilon\xi}{L_c}\right)^2. \quad (12)$$

This formula shows that and how  $H_{dis}(T)$  approaches  $H_{c2}(T)$ , which is also seen in Fig. 1. Interestingly, according to this formula, the order-disorder transition occurs *outside* the upper region of single vortex pinning<sup>36</sup>, but its position correlates with the boundary of this region:  $[1 - h_{dis}(t)]/[1 - h_{sv}(t)] = (2\pi c_L^2)^{-2/3} > 1$ . It should be also noted that in the case under study (i.e. when the thermal fluctuations are negligible) the mean-field  $H_{c2}(T)$  practically coincides<sup>37</sup> with the melting line  $H_m(T)$ . Thus, we obtain for  $D > c_L$  that in the high temperature region a peak effect occurs near the melting line, while with decreasing  $T$  the position of the peak in  $j_c(H)$  shifts downwards from this line. This situation is reminiscent of that of perfect high- $T_c$  superconductors.<sup>10-16</sup>

In this context it is also useful to note the following: The density of the dislocations in the vortex liquid is essentially higher than in the disordered vortex solid phase

near the order-disorder transition.<sup>22</sup> However, if in the  $H - T$  plane the order-disorder transition occurs sufficiently below the melting line of the clean superconductor, then in the disordered solid phase, at the field corresponding to the melting transition, the density of the dislocations generated by the quenched disorder may become of the order of the density characteristic for the liquid phase. In this case the melting transition *disappears*. In other words, the melting line  $H_m(T)$  terminates when  $H_{dis}(t)$  deviates from it appreciably.

If the strength of the disorder is sufficiently small,

$$D \equiv \frac{\epsilon\xi(0)}{L_c(0)} < c_L,$$

the order-disorder line lies entirely outside the region of single vortex pinning, Fig. 2, and is described by Eq. (9) at any  $T < T_c$ , while Eq. (4) is not valid at all. In the special situation when  $D$  is markedly less than  $c_L$ , a peak effect occurs near  $H_{c2}(T)$  and its position in the  $H - T$  plane is approximately given by Eq. (12). In this case the resulting phase diagram looks like that of low- $T_c$  superconductors.<sup>1-5</sup> The transition from one type of phase diagram to the other occurs when  $D = c_L$ .

It has been assumed in this section that the parameter  $\epsilon\xi/L_c$  decreases with increasing  $T$ . However, the  $\delta T_c$  pinning (due to spatial variations of  $T_c$ ) leads to an increasing function  $g_0(t)$ , see Eq. (A14) in Appendix A. In this case, if  $D > c_L$ , the formula (4) remains valid up to  $T_c$ . But if  $D < c_L$ , a temperature  $T_0$  exists, determined by the condition

$$\frac{\epsilon\xi(T_0)}{L_c(T_0)} = c_L,$$

and at  $T < T_0$  equation (9) should be used, while at  $T > T_0$  formula (4) holds. In other words, we have a situation which is opposite to that described above. In Fig. 3 the order-disorder line is shown for the case when  $g_0(t)$  is given by Eq. (A14). Note that in this case, according to formula (4), one has  $H_{dis} \propto (1 - t^2)^{3/2}$  in the high temperature region of the phase diagram. This result qualitatively agrees with the measurements<sup>6-9,11,16</sup> on  $\text{YBa}_2\text{Cu}_3\text{O}_{7-\delta}$  crystals when  $\delta$  is not small, or when the crystals are not too perfect.

### IV. THE ORDER-DISORDER LINE WITH ACCOUNT OF THERMAL FLUCTUATIONS

It is well-known that thermal fluctuations of the flux-line lattice play an important role in high- $T_c$  superconductors. In particular, for this reason the flux-line lattice melts essentially below the mean-field  $H_{c2}$  line. In this section we study the influence of thermal fluctuations on the order-disorder line.

Thermal fluctuations lead to a smoothing of the pinning potential and thus increase the Larkin length  $L_c$ .

The length  $L_c$  specifies the boundary of the single vortex pinning region and it enters the key parameter of the collective pinning theory,  $\epsilon\xi/L_c$ . Here we reserve the notation  $L_c$  for the true length renormalized by the fluctuations, while the Larkin length defined without account of the fluctuations will be denoted below as  $L_c^0$ . Note that just  $L_c^0$  has been used in Sec. III, and just this quantity is described by Eq. (10). Apart from increasing  $L_c$ , the thermal fluctuations of the flux-line lattice also modify the correlation function (3) as follows<sup>27</sup>:

$$u^2(0, L_0) \approx r_p^2(L_0/L_c)^{2\zeta}, \quad (13)$$

where  $r_p^2 = \xi^2 + u_T^2$ , and  $u_T$  is the magnitude of these fluctuations, which depends on the temperature and on the magnetic field. It is implied in Eq. (13) that  $L_0 = \epsilon a > L_c$ . As to the correlation function (8), the collective pinning theory<sup>27</sup> gives

$$u^2(a, 0) \approx \xi^2(L_0/L_c^0)^3 \left( \frac{1 - h_{sv}}{1 - h} \right)^{3/2} \left( \frac{\xi}{r_p} \right)^4 \quad (14)$$

for  $L_0 < L_c$ , i.e. at  $h > h_{sv} = 2\pi(\epsilon\xi/L_c)^2$ .

Since  $u(a, 0) = u(0, L_0)$ , the correlation functions (13) and (14) must coincide at  $L_0 = L_c$  (or equivalently at  $h = h_{sv}$ ). This condition yields

$$L_c(t) = L_c^0(t) \frac{r_p^2(t, H_{sv}(t))}{\xi^2(t)}. \quad (15)$$

In fact, formula (15) is an *equation for  $L_c$*  since we have the relationship  $H_{sv} = \Phi_0 \epsilon^2 / L_c^2$ . This equation enables us to find  $L_c(t)$ , and thus  $H_{sv}(t)$ , self-consistently.

To proceed, we have to estimate the magnitude of thermal displacements of the lattice,  $u_T$ , relative to its equilibrium position. In the case of the *ideal* vortex lattice,  $u_T$  was calculated in many papers; see, e.g., Refs. 38–40. This magnitude, as well as the correlation functions (8) and (14), depends on the elastic moduli of the lattice. However, in deriving Eqs. (8), (14) the contribution associated with the compression modulus  $c_{11}$  was neglected. Hence, it is consistent to use the same approximation in the calculation of  $u_T^2$ . This simplifies the appropriate formula<sup>40</sup> for  $u_T^2$ , and we obtain

$$u_T^2 \approx \xi^2 t \left( \frac{Gi}{1 - t^2} \right)^{1/2} h^{-1/2} f(h), \quad (16)$$

where  $h = H/H_{c2}(t)$ ,  $t = T/T_c$ ,  $H_{c2}(t) = H_{c2}(0)(1 - t^2)$ ,  $Gi$  is the Ginzburg number,

$$Gi = \frac{1}{2} \left( \frac{T_c}{H_{c2}^2(0)\epsilon\xi^3(0)} \right)^2,$$

which characterizes the strength of the thermal fluctuations, and  $H_c$  is the thermodynamic magnetic field of the superconductor. The function  $f(h)$  has the form:

$$f(h) = \frac{2\beta_A}{1 - h} \frac{[1 + (1 + \tilde{c})^2]^{1/2} - 1}{\tilde{c}(1 + \tilde{c})}, \quad (17)$$

with  $\tilde{c} = 0.5[\beta_A(1 - h)]^{1/2}$ , and  $\beta_A = 1.16$ .

The quenched disorder changes  $u_T^2$ . However, when the transverse collective pinning length  $R_c$  is considerably greater than  $a$ , the above result for the ideal lattice is a good approximation. This is due to the fact that the main contribution to  $u_T$  results from the thermal fluctuations with short wavelengths ( $k_\perp \sim 1/a$ ), while the quenched disorder essentially distorts the lattice only on the scale  $R_c$ . Thus, we may use Eq. (16) in the case of the *nonideal* lattice if bundle pinning occurs. But in the single vortex pinning regime the influence of the disorder is essential, and one has<sup>27</sup>  $u_T^2 \propto L_c$ . To account for this result, we introduce an additional factor  $L_c/\epsilon a$  in the formula (16) and thus obtain

$$u_T^2 \approx \xi^2 t \left( \frac{Gi}{1 - t^2} \right)^{1/2} h_{sv}^{-1/2} f(h) \quad (18)$$

in the single vortex pinning region at  $h < h_{sv}$ .

Inserting expression (16) into formula (15) and using definition (10) for  $\epsilon\xi/L_c^0$ , we obtain the following equation for  $h_{sv} = H_{sv}/H_{c2}$ :

$$h_{sv}^{1/2}(t) = (2\pi)^{1/2} D g_0(t) - t \left( \frac{Gi}{1 - t^2} \right)^{1/2} f(h_{sv}(t)). \quad (19)$$

With increasing  $t$  the function  $h_{sv}(t)$  reaches zero at some  $t_{dp}^s < 1$ , and Eq. (19) is valid at  $t \leq t_{dp}^s$ . In the region  $t > t_{dp}^s$  the length  $L_c$  is infinite in size, and the single vortex pinning regime is absent, i.e.,  $h_{sv}(t) = 0$  at  $t > t_{dp}^s$ . The value of  $t_{dp}^s$  is found by equating  $h_{sv}$  to zero in formula (19):

$$t_{dp}^s = \frac{(2\pi)^{1/2} D}{Gi^{1/2} f(0)} g_0(t_{dp}^s) [1 - (t_{dp}^s)^2]^{1/2}. \quad (20)$$

It may be verified that the right hand side of Eq. (20) coincides (up to a numerical factor of the order of unity) with the dimensionless characteristic pinning energy  $\tilde{T}_{dp}^s/T_c$ , see Appendix A. Thus, in agreement with physical considerations,<sup>27</sup> we obtain that the essential renormalization of  $L_c$  occurs at such temperatures  $T$  that  $T \sim \tilde{T}_{dp}^s(T)$ .

It should be noted that our result for  $L_c$  ( $L_c \rightarrow \infty$  at  $t \rightarrow t_{dp}^s$ ) differs in some respects from that presented in Ref. 27 where  $L_c$  increases exponentially at  $t \sim t_{dp}^s$ . However, in the framework of our approximation,  $H_{c1} = 0$ , we may consider  $L_c$  as infinite if it becomes of the order of  $\lambda$ . Hence, the difference between the results is, in fact, small. But our approach provides the continuity of the correlation functions (13), (14) at  $h = h_{sv}$ .

Equation (19) specifies the single vortex pinning (SVP) region existing at relatively low magnetic fields [ $0 < h < h_{sv}(t)$ ]. However, formulas (14), (16) enable one to find also the upper region in which the vortex system returns

to this type of pinning again. The appropriate equation results from the condition  $u(a, 0) = r_p$ , and has the following form:

$$(1 - h) \left[ h^{1/2} + t \left( \frac{Gi}{1 - t^2} \right)^{1/2} f(h) \right]^2 = 2\pi (Dg_0(t))^2 [1 - h_{sv}(t)], \quad (21)$$

As might be expected, at  $h = h_{sv}$  this equation goes over into Eq. (19). However, in a certain temperature interval it has two additional real roots which form the boundary of the upper SVP region,  $h_{sv}^{up}$  (see Fig. 5 below). Here we do not consider this issue in detail, but qualitatively describe the effect of thermal fluctuations on the shape of the upper SVP region specified above without their account.<sup>36</sup> Although the softening of the vortex lattice near  $H_{c2}$  is favorable for single vortex pinning, this softness also leads to an increase of the thermal fluctuations  $u_T$ , which reduces the strength of pinning. As a result, the upper region does not touch  $H_{c2}(t)$  except for the point  $t = 0$  (at  $t > 0$  and  $H = H_{c2}$  we have  $u_T = \infty$ ). Besides this, since  $u_T$  increases with  $t$ , the upper region does not extend to  $T_c$ . Of course, one should realize that the part of the boundary of this SVP region lying above the vortex lattice melting curve has only formal meaning, since it does not account for the vanishing shear modulus at the melting. On the other hand, it is quite possible that the sharp melting transition disappears when the melting line enters the upper SVP region (or even before it; see Sec. V).

Inserting expressions (13) and (18) in formula (2), we arrive at an equation for  $h_{dis} = H_{dis}/H_{c2}$  which generalizes formula (4):

$$h_{dis} \left[ 1 + t \left( \frac{Gi}{1 - t^2} \right)^{1/2} \frac{f(h_{dis})}{(h_{sv}(t))^{1/2}} \right]^{1/(1-\zeta)} = 2\pi c_L^2 \left( \frac{2\pi c_L^2}{h_{sv}(t)} \right)^{\alpha/2}. \quad (22)$$

This equation is valid in the single vortex pinning regime when  $h_{dis} \leq h_{sv}$ . For example, if  $g_0(t)$  is a decreasing function of  $t$ , the order-disorder line lies in the single vortex pinning region and is described by Eq. (22) at  $t < t_1$ . In the case  $D > c_L$  the temperature  $t_1$  is found from the equation:

$$h_{sv}(t_1) = 2\pi c_L^2 \left[ 1 + t \left( \frac{Gi}{1 - t^2} \right)^{1/2} \frac{f(h_{sv}(t))}{(h_{sv}(t))^{1/2}} \right]_{t=t_1}^{-1}, \quad (23)$$

which generalizes condition (6). At  $D < c_L$  the line is entirely outside this region, and thus one has  $t_1 = 0$ . If  $g_0(t)$  is an increasing function of temperature, more complicated situations can occur.

Inserting formulas (14) and (16) into relation (1), we obtain the equation for  $h_{dis}(t)$ :

$$h_{dis}(1 - h_{dis})^3 \left[ 1 + t \left( \frac{Gi}{1 - t^2} \right)^{1/2} \frac{f(h_{dis})}{(h_{dis})^{1/2}} \right]^4 = 2\pi c_L^2 \left( \frac{Dg_0(t)}{c_L} \right)^6 [1 - h_{sv}(t)]^3, \quad (24)$$

which generalizes Eq. (9). This equation is valid in the bundle pinning region.

Let us now present formulas for the melting line which is determined by the Lindemann criterion,  $u_T^2 = c_L^2 a^2$ , different from Eqs. (1), (2). This well-known empirical criterion based on the magnitude of the thermal fluctuations, was justified in Ref. 22 for the case of the ideal vortex lattice. According to this paper, different physical mechanisms lead to the proliferation of dislocations at the vortex lattice melting and at the order-disorder transition. While the disorder-induced transition is driven by an adjustment of the flux-line lattice to the disorder, the thermal melting is governed by the entropy gain associated with the creation of dislocations. Hence, the Lindemann constant  $c_L$  for the melting may, in principle, differ from that used in Eqs. (22)-(24). However, for the sake of simplicity we take these constants  $c_L$  as equal in the following analysis. Thus, if the melting line  $h_m(t) = H_m/H_{c2}$  does not intersect  $h_{sv}(t)$ , it is described by the equation:

$$t \left( \frac{Gi}{1 - t^2} \right)^{1/2} h_m^{1/2} f(h_m) = 2\pi c_L^2. \quad (25)$$

But if the melting line lies below  $h_{sv}(t)$ , an additional factor  $(h_m/h_{sv})^{1/2}$  should be inserted on the left hand side of Eq. (25), cf. Eqs. (16) and (18). Finally, we note that in expression (25), as well as in Eqs. (16), (18)-(24), the factor  $1 - t^2$  represents the temperature dependence of the upper critical field,  $1 - t^2 = H_{c2}(t)/H_{c2}(0)$ . Thus, if another form of this dependence is implied, the appropriate modification of all these equations is straightforward.

Summing up, we may state the following: For given  $g_0(t)$ , equations (19)-(25) enable us to calculate the order-disorder line  $h_{dis}(t)$ , the melting line  $h_m(t)$  and the boundaries of the single vortex pinning regime  $h_{sv}(t)$ ,  $h_{sv}^{up}(t)$  with account of the thermal fluctuations. The function  $g_0(t)$  in Eq. (10) is determined by the pinning mechanism and by the temperature dependences of  $\xi$  and  $\lambda$ , see Appendix A.

## V. ANALYSIS OF PHASE DIAGRAMS

It is important to emphasize that for given  $g_0(t)$  Eqs. (19)-(25) depend only on *two* parameters: the strength of quenched disorder,  $D = \epsilon\xi(0)/L_c(0)$ , and the strength of the thermal fluctuations,  $Gi$ . In this sense, the equations and figures of Sec. III correspond to the limiting case  $Gi \rightarrow 0$ . We consider now new features of the phase diagram which appear in the real situation of finite  $Gi$ .

## A. Numerical results

An example of the phase diagram in the case  $D > c_L$  is shown in Fig. 4. Note that the order-disorder line terminates at some temperature  $t_e < 1$ . This termination is associated with an increase of the thermal fluctuations and thus with an enhanced smoothing of the pinning potential when the order-disorder line approaches  $H_{c2}$ . Interestingly, the end point lies near the so-called depinning line<sup>27,41</sup> where  $u_T^2 = \xi^2$ . Another new feature of the phase diagram is the intersection of the melting and the order-disorder lines. Thus, we obtain the point where both lines merge. It is seen from Fig. 4 that at this point the position of the critical current peak begins to shift sharply downward from the melting curve, in agreement with the experimental data.<sup>10–16</sup> Hence, as was mentioned in Sec. III C, the upper critical point for the melting is likely to occur somewhere nearby. The portion of the order-disorder line lying above the melting curve has no physical meaning since the density of dislocations in the liquid phase is already higher than in the disordered solid phase.<sup>22</sup> Note also that the rise of  $H_{dis}(t)$  at  $T > T_1$  becomes considerably steeper than in the case  $Gi = 0$ .

The intersection of the order-disorder line with the melting curve occurs also for  $D < c_L$ . In this case, when  $Gi$  increases, the decrease of  $H_{dis}$  with  $T$  diminishes, and eventually  $H_{dis}$  becomes an increasing function of  $t$ , see Fig. 5. Therefore, if  $Gi \sim 10^{-2}$  (this value is typical for YBaCuO crystals), the temperature behavior of the order-disorder line is similar to that obtained for  $D > c_L$ , and the phase diagrams in both these cases are of the same type.

In Fig. 5 we also show the upper region of single vortex pinning. It is important to note that the intersection point of the order-disorder line and the melting line occurs clearly *before* the melting curve enters this region, and so at the intersection point the transverse collective pinning length  $R_c$  and the positional correlation length  $R_a$  (the dislocation spacing) both considerably exceed the flux-line spacing  $a$ . This fact justifies the assumed weak influence of quenched disorder on the vortex lattice melting and the application of Eq. (24) up to the intersection point.

If the parameter  $D$  increases, e.g., as a result of irradiation or of reduction of the oxygen content in YBa<sub>2</sub>Cu<sub>3</sub>O<sub>7- $\delta$</sub>  crystals (see Appendix A), then the order-disorder line shifts down, while the temperature of the intersection point (and thus the temperature of the upper critical point for the melting line) increases, Fig. 6. These results are in agreement with the experimental findings<sup>10,11,15,16</sup> for YBa<sub>2</sub>Cu<sub>3</sub>O<sub>7- $\delta$</sub>  crystals. However, although the obtained results qualitatively describe the phase diagram of these crystals and its evolution with varying  $D$ , it should be emphasized that the intersection point does not reach  $T_c$  at reasonable values of the disorder parameter  $D$ .

Consider now the case when  $g_0(t)$  increases with  $t$ . This situation occurs in the model of  $\delta T_c$  pinning, see Appendix A. The appropriate phase diagrams are presented in Figs. 7-9. It is important to note the following: At sufficiently strong disorder, the line  $H_{dis}(t)$  monotonically decreases with temperature and practically reaches  $T_c$ . When the strength of the disorder decreases, the order-disorder line exhibits nonmonotonic behavior with  $t$ , and the temperature of the intersection point,  $t_i$ , goes down. Thus, in contrast to the case of a decreasing function  $g_0(t)$ , the model of  $\delta T_c$  pinning correctly reproduces all the features of the experimental data for YBa<sub>2</sub>Cu<sub>3</sub>O<sub>7- $\delta$</sub>  crystals.<sup>6–16</sup> In particular, the results presented in Fig. 8 closely resemble the development of the order-disorder line with variations of the oxygen deficiency  $\delta$ , see, e.g., Fig. 9 in Ref. 11.

The results of this section may also provide an explanation of the findings obtained in Ref. 18. It was shown in this paper that the flux-line pinning in pure YBa<sub>2</sub>Cu<sub>3</sub>O<sub>7- $\delta$</sub>  crystals is mainly due to a nonuniform distribution of oxygen vacancies over the sample. Changing the conditions of annealing of the sample, Erb et al. changed this distribution at a fixed  $\delta$ . When the distribution became more homogeneous, the fishtail effect disappeared. Since the spatial fluctuations in the density of oxygen vacancies strengthen the  $\delta T_c$  pinning, we get an additional confirmation of the hypothesis that this type of pinning plays the main role in not too perfect YBaCuO crystals, and so the fishtail effect exists up to high temperatures, as shown in Figs. 7, 8 for large  $D$ . When, after annealing, the crystal becomes more perfect, and the above-mentioned spatial fluctuations are reduced, the value of the parameter  $D$  appears to decrease considerably. (Moreover, it is conceivable that some other type of pinning begins to dominate.) Thus, we arrive at the situation when a fishtail effect is absent, at least in the region of not too high magnetic fields, as it follows from the data shown in Figs. 6 and 8 for small  $D$ .

Finally, we briefly describe the case of small Ginzburg numbers which occurs for conventional superconductors. In this case the temperatures  $t_{dp}^s$  and  $t_i$  are practically equal to unity, the melting line almost coincides with  $H_{c2}(t)$ , and the phase diagrams tend to those shown in Figs. 1-3. Thus, the results of the simplified approach of Sec. III can be well applied to such superconductors.

## B. Approximate formulas. Discussion

We now present analytical results which give some insight into the origin of the above-mentioned features of the phase diagrams. Let us start with the melting line. If  $[Gi/(1-t^2)]^{1/2} \ll 2\pi c_L^2$ , the normalized field  $h_m = H_m/H_{c2}$  is close to unity, and we obtain from Eq. (25)

$$1 - h_m \approx \left( \frac{f_1(1)}{2\pi c_L^2} \right)^{2/3} t^{2/3} \left( \frac{Gi}{1-t^2} \right)^{1/3}, \quad (26)$$

where

$$f_1(h) \equiv (1-h)^{3/2}f(h)$$

is defined through the function  $f(h)$  given by Eq. (17), with  $f_1(1) \approx 1.78$ . Equation (26) agrees with the strict result<sup>37</sup> derived for clean superconductors without using the Lindemann criterion. Formula (26) expressed in usual units ( $H_m = h_m H_{c2}$ ) means that

$$H_{c2}(t) - H_m(t) \propto Gi^{1/3}(1-t^2)^{2/3}.$$

The right hand side of this expression is the width of the fluctuation region in not too small magnetic fields,<sup>42,43</sup>  $h \gg Gi$ . In the opposite limiting case when  $f_1(0)[Gi/(1-t^2)]^{1/2} \gg 2\pi c_L^2$  [but the temperature is outside the critical region for zero magnetic field,  $Gi < (1-t^2)$ ], the field  $h_m$  is small, and Eq. (25) yields:

$$h_m = \left( \frac{2\pi c_L^2}{f_1(0)t} \right)^2 \frac{1-t^2}{Gi}, \quad (27)$$

where  $f_1(0) \approx 2.34$ . In fact, this is the well-known result<sup>27,38-40</sup> for clean superconductors,

$$H_m \propto (1-t)^2.$$

Note that for Eq. (27) to hold in a sufficiently wide temperature region, the Ginzburg number should not be too small. Finally, we point out an interesting feature of Eq. (25) that follows from our numerical analysis. The formula

$$H_m = A(1-t^2)^\gamma, \quad (28)$$

with some constants  $A$  and  $\gamma$  turns out to give a very good fit to  $H_m(t)$  determined by Eq. (25) in the wide temperature interval  $0.5 < t < 0.98$ , see Fig. 10. The values of the parameters  $A$  and  $\gamma$  depend on  $Gi$ , and the exponent  $\gamma$  increases with increasing  $Gi$ . In particular, we find  $1.24 < \gamma < 1.59$  when  $0.001 < Gi < 0.01$ . In this connection it is worth noting that formulas of the type of Eq. (28) are widely used to approximate experimental data, and frequently an exponent  $\gamma \approx 4/3$  is found, which is characteristic for the fluctuation region of a 3D XY-type phase transition. We emphasize here that a good fit by such formulas does not necessarily mean the existence of a large fluctuation region in zero magnetic field, but may result from the specific form of the expression [Eq. (25)] describing the melting line.

In the case of  $\delta T_c$  pinning the melting line may lie inside the region of single vortex pinning, i.e. the inequality  $h_{sv} > h_m$  may hold. This occurs if the parameter  $\nu$  (see Ref. 27, p. 1218),

$$\nu \equiv \frac{(2\pi)^{3/2} D^3}{Gi^{1/2}}, \quad (29)$$

is sufficiently large,  $\nu^{1/3} \gg 1$ . Although in this case the shape of the melting line requires a special investigation

and is not discussed in detail here, it should be realized that the sharp melting transition may disappear in this region.

Let us now analyze Eq. (24) which describes the line  $h_{dis}(t)$  in the region  $h > h_{sv}$ . To understand the behavior of this line, we note the following: The function  $f_1(h) = (1-h)^{3/2}f(h)$  decreases monotonically with increasing  $h$ ; its variation in the interval  $0 < h < 1$  is not large,  $f_1(1)/f_1(0) \approx 0.76$ , and so if one considers  $f_1(h)$  as constant,  $f_1(h) = f_1(0) \equiv f_1 \approx 2.34$ , this leads to a sufficiently accurate approximation in solving Eq. (24). In this approximation Eq. (24) becomes a quadratic equation in the variable  $h_{dis}^{1/2}(1-h_{dis})^{3/2}$ , and its solution has the form:

$$h_{dis}^{1/2}(1-h_{dis})^{3/2} = F_D - F_T + [(F_D - F_T)^2 - (F_T)^2]^{1/2} \quad (30)$$

where  $F_D$  and  $F_T$  are the following functions of temperature:

$$F_D(t) = \frac{(2\pi)^{1/2}[Dg_0(t)]^3}{2c_L^2} [1 - h_{sv}(t)]^{3/2},$$

$$F_T(t) = f_1 t \left( \frac{Gi}{1-t^2} \right)^{1/2}.$$

At  $t = 0$  we have  $F_T(0) = 0$ , and equation (30) goes over into Eq.(9). Thus, the effect of thermal fluctuations is reduced to a *renormalization* of the right hand side of Eq. (9) [including the change of the function  $h_{sv}(t)$  according to Eq. (19)]. Note that the magnitude of this renormalization (i.e., the ratio  $F_T/F_D$ ) is mainly determined by the parameter  $\nu^{-1}$ , see Eq. (29). Interestingly, in contrast to the case of the  $\delta T_c$  pinning where  $\nu$  appears as a result of the specific temperature dependence of  $g_0$ , Eq. (A14), we now conclude that the parameter  $\nu$  characterizes the relative strength of pinning of any type.

It should be emphasized that the right hand side of Eq. (30) is real only if  $F_D \geq 2F_T$ . Thus, we find that the order-disorder line terminates at a temperature  $t_e$  which satisfies the equation

$$F_D(t_e) = 2F_T(t_e). \quad (31)$$

Taking into account Eqs. (16) and (31), it is easy to determine the ratio  $u_T^2/\xi^2$  at the end point of the order-disorder line,  $t = t_e$ ,  $h = h_{dis}(t_e)$ :

$$\frac{u_T^2}{\xi^2} = F_T(t_e)h^{-1/2}(1-h)^{-3/2} = \frac{F_T(t_e)}{F_T(t_e)} = 1.$$

Hence, this end point lies on the so-called depinning line<sup>27</sup> defined by the condition  $u_T^2 = \xi^2$ , see Figs. 4, 5. It can be also verified that  $t_e$  is always less than the temperature  $t_{dp}^s$  determined by Eq. (20).

As has already been mentioned above, only the intersection point of the melting and the order-disorder lines has a physical meaning rather than the end point



of  $H_{dis}(t)$ . The temperature of this intersection point,  $t_i$ , can be simply estimated using formulas (26) and (30). Then we arrive at the following equation for  $t_i$ :

$$4\pi c_L^2 F_D(t_i) = (1 + 2\pi c_L^2)^2 F_T(t_i),$$

or explicitly,

$$t_i = \nu \frac{[g_0(t_i)]^3 (1 - t_i^2)^{1/2} [1 - h_{sv}(t_i)]^{3/2}}{f_1 (1 + 2\pi c_L^2)^2}. \quad (32)$$

This equation suggests that the temperature of the intersection point,  $t_i$ , depends on the parameters  $Gi$  and  $D$  mainly through their combination  $\nu$ , Eq. (29). The data of Fig. 11 support this hypothesis, viz., at given  $g_0(t)$  the temperatures  $t_i$  calculated for various  $Gi$  fall on the same curve. Of course, this prediction, as well as any *quantitative* conclusion based on Eqs. (19)-(25), requires an experimental verification since a number of simplifying assumptions were made above. In particular,  $c_L$  was assumed to be the same constant for the melting and for the order-disorder transition in all the pinning regimes. On the other hand, according to Eq. (32), the dependence of  $t_i$  on  $c_L$  is relatively weak.

Since  $t_i$  specifies the width of the temperature region where the order-disorder transition exists, the data of Fig. 11 mean that this width is characterized by the parameter  $\nu$ . These data also shed light on the different behavior of  $H_{dis}(t)$  in Figs. 6 and 8 at large values of  $D$ . To elucidate the results of Fig. 11 and the conclusions made on their basis, let us analyze Eq. (32) in two limiting cases. If  $\nu \ll 1$ , one obtains the following estimate from this equation:

$$t_i \approx 0.42(1 + 2\pi c_L^2)^{-2} \nu.$$

In other words, we have a situation qualitatively similar to that shown in Fig. 6 or in Fig. 8 for the smallest  $D$ . In this case the order-disorder transition occurs only at very low temperatures  $t < t_i$ , while the portion of the melting line at  $t > t_i$  has a large extension. Note that, according to the estimates of  $Gi$  and  $D$  presented in Ref. 2, such a situation must take place in pure crystals of 2H-NbSe<sub>2</sub>, which were investigated in numerous papers. This conclusion does not contradict the observation of a peak effect in these crystals,<sup>2</sup> since a peak effect can signalize not only the order-disorder transition, as it has been implied so far, but also the vortex lattice melting.<sup>44-48</sup> Of course, the features of the peak effect may differ in these two cases.

In the opposite limit,  $\nu \gg 1$ , the order-disorder transition reaches  $T_c$ , while the region of “pure” melting ( $t_i < t < 1$ ) is contracted. This limit just corresponds to conventional superconductors for which  $Gi \ll 1$ , see Figs. 1-3. However, in the process of approaching this limit, the evolution of the phase diagram is different for the different models of pinning, i.e., in the cases of Eqs. (A13) and (A14). That is why Figs. 6 and 8 differ

from each other at large values of  $D$ . If Eq. (A13) is valid, one finds from Eq. (32) that

$$1 - t_i^2 \approx 1.5(1 + 2\pi c_L^2) \nu^{-1/2}.$$

Thus, a large  $\nu$  is required for the temperature  $t_i$  to reach unity, see Fig. 6. In the case of Eq. (A14) the right hand side of Eq. (32) already exceeds unity at a finite value  $\nu$  ( $\nu \sim 1$ ), and at such  $\nu$  the line  $H_{dis}(t)$  practically reaches the point  $T = T_c$ ,  $H = 0$ , see Fig. 8 for the largest  $D$ .

### C. Upper critical point.

Let us now discuss the upper critical point on the vortex lattice melting curve.<sup>17</sup> In principle, two scenarios are possible. In the first one<sup>22</sup> the upper critical point does not coincide with the intersection point of the melting and the order-disorder lines and is located at a higher magnetic field than this intersection point. In fact, in this case the intersection of the *two different* phase transition lines occurs, and one of them (the order-disorder line) terminates at the intersection while the other one continues for some distance which seems to depend on the detailed position of the lines in the  $H-T$  plane. This scenario is based on the difference in the density of dislocations,  $\rho$ , generated at the melting and the order-disorder transition: at the melting one has  $\rho \sim a^{-2}$ , while at the order-disorder transition  $\rho \sim R_a^{-2} \ll a^{-2}$ . The position of the upper critical point on the melting line is determined by the condition that the density of dislocations in the disordered vortex solid phase reaches a value typical for the liquid (i.e., the dislocation spacing  $R_a$  calculated on the melting curve reduces to the vortex spacing  $a$ ). It is this scenario that is assumed in our paper.

In the second scenario the upper critical point coincides with the intersection point. In this case the above-mentioned point is ordinary rather than singular for the free energy of the vortex system, since a continuous phase transition separating the disordered vortex solid phase from the vortex liquid does not seem to exist.<sup>49,50</sup> Thus, there is only *one* phase transition line which describes both the melting and the order-disorder transitions. This unified line originates from the melting curve of clean superconductors, gradually evolving from it as the strength of the quenched disorder increases. The “upper critical point” is then simply the point where on the melting line  $R_a$  reduces to  $a$  and the line experiences a bend. However, for this scenario to occur, the calculated intersection point must lie in the single vortex pinning region. Otherwise, one obtains  $R_a > R_c \gg a$  at this point and returns to the first scenario.

Our results argue in favor of the first scenario since *in the framework of the used approximations* the intersection points never reach the upper region of single vortex pinning (see, e.g., Fig. 5). Note that this scenario is also supported by recent numerical simulations.<sup>51</sup>

## VI. CONCLUSIONS

In this paper, using the Lindemann criterion and results of the collective pinning theory,<sup>27</sup> we have derived equations (19)-(25) which enable one to calculate the order-disorder transition line  $H_{dis}(t)$  with account of both pinning-caused and thermal fluctuations in the whole temperature interval of its existence. The boundaries of the single vortex pinning region,  $H_{sv}(t)$ ,  $H_{sv}^{up}(t)$ , and the melting line  $H_m(t)$  are also found from these equations. The equations turn out to depend only on the Ginzburg number  $Gi$  which characterizes thermal fluctuations, on the strength of the quenched disorder,  $D$ ,

$$D = \frac{\epsilon\xi(0)}{L_c(0)} = \left( \frac{j_c(0)}{j_0(0)} \right)^{1/2},$$

and on the function  $g_0(t)$  defined by the pinning mechanism and by the temperature dependences of  $\xi$  and  $\lambda$ , Appendix A. For example, the pinning mechanism considered in Ref. 52 leads to a  $g_0(t)$  described by Eq. (A13), while the  $\delta T_c$  pinning<sup>27</sup> results in Eq. (A14). Using our equations one can analyze the phase diagrams of various superconductors. Moreover, our analysis in principle allows to obtain information on the true form of the function  $g_0(t)$ , i.e., on the mechanism of pinning in a superconductor.

At small  $Gi$  we obtain phase diagrams typical for low- $T_c$  superconductors. In this case the obtained results practically coincide with the results of the simplified approach presented in Sec. III. We also analyze phase diagrams with  $Gi \sim 10^{-2}$  since such values of  $Gi$  are characteristic for the  $\text{YBa}_2\text{Cu}_3\text{O}_{7-\delta}$  superconductors. We consider both a typical case where  $g_0(t)$  decreases with  $t$  [Eq. (A13)] and a case where  $g_0(t)$  increases with  $t$  [Eq. (A14)]. In both these cases the obtained results qualitatively describe the phase diagram of  $\text{YBaCuO}$  crystals and its evolution with varying  $D$ , which can be caused by irradiation or by reduction of the oxygen content in these crystals. However, we find that the model of  $\delta T_c$  pinning [Eq. (A14)] more correctly reproduces all the features of the experimental data for  $\text{YBa}_2\text{Cu}_3\text{O}_{7-\delta}$  crystals.

Our results support the idea<sup>22</sup> that the upper critical point on the melting curve of high- $T_c$  superconductors does not generally coincide with the intersection point of the melting and the order-disorder lines (although the distance between them is possibly small). We predict the position of this intersection point in the  $H-T$  plane. We suppose that the temperature corresponding to this point is determined mainly by the parameter  $\nu$ , Eq. (29), i.e., by a combination of the parameters  $D$  and  $Gi$ .

## ACKNOWLEDGMENTS

G.P.M. acknowledges the hospitality of the Max-Planck-Institut für Metallforschung, Stuttgart. E.H.B.

wishes to acknowledge the hospitality of the Institute for Superconducting and Electronic Materials, University of Wollongong, Australia, where part of this work was performed, and financial support from the Australian Research Council, IREX Program.

## APPENDIX A: ESTIMATES OF THE PARAMETERS

The results of this paper are based on the collective pinning theory.<sup>27,32</sup> It is assumed in this theory that the disorder in the flux-line lattice is generated by point defects of size not exceeding the coherence length  $\xi(0)$ . Here, in the framework of three widely used models of pinning, we express the quantities  $\epsilon\xi/L_c$  and  $\tilde{T}_{dp}^s$  through the characteristics of the point defects, viz., their concentration  $n$  and mean radius  $r_0$ . These expressions enable us to get some idea of the temperature dependences of these quantities and to understand the changes of the phase diagram when  $n$  and  $r_0$  are varied.

In the first model,<sup>53</sup> pinning is due to the gain in the condensation energy when a vortex core is located at a defect. This gain  $\epsilon_{pin}$  is of the order  $(H_c^2/8\pi)4\pi r_0^3/3$ , where  $H_c$  is the thermodynamic magnetic field and  $r_0$  the radius of the defect. Then one obtains the following estimates for the mean elementary pinning force exerted by one point defect  $f_{pin} \sim \epsilon_{pin}/\xi$ :

$$f_{pin} \approx \epsilon_0 \left( \frac{r_0}{\xi} \right)^3, \quad (\text{A1})$$

and for the single vortex collective pinning length<sup>27</sup>  $L_c = n^{-1/3}(\epsilon^2\epsilon_0/f_{pin})^{2/3}$  [with  $\epsilon = \lambda_{ab}/\lambda_c$ ,  $\epsilon_0 = (\Phi_0/4\pi\lambda_{ab})^2$ ]:

$$L_c \approx \frac{\epsilon^{4/3}}{n^{1/3}} \left( \frac{\xi}{r_0} \right)^2. \quad (\text{A2})$$

Using these estimates, we find the key parameter (7),

$$\frac{\epsilon\xi}{L_c} \approx \left( \frac{nr_0^3}{\epsilon} \right)^{1/3} \frac{r_0}{\xi}, \quad (\text{A3})$$

and the characteristic pinning energy<sup>27</sup>  $\tilde{T}_{dp}^s$  described by the expression  $\xi(f_{pin}^2 n L_c \xi^2)^{1/2}$ ,

$$\tilde{T}_{dp}^s \approx \epsilon^{2/3} \epsilon_0 (nr_0^3)^{1/3} r_0. \quad (\text{A4})$$

A different mechanism of pinning is due to the scattering of quasiparticles by the defect as calculated in Ref. 52. A scattering center facilitates deformations of the order parameter up to distances of the order of the zero-temperature coherence length  $\xi(0)$ . Hence, it is energetically advantageous for a vortex core to sit at a scattering center. This mechanism leads to the pinning force  $f_{pin} \sim (H_c^2/8\pi)r_0^2\xi(0)/\xi$ , and we obtain

$$f_{pin} \approx \varepsilon_0 \left( \frac{r_0}{\xi} \right)^2 \frac{\xi(0)}{\xi}, \quad (\text{A5})$$

$$L_c \approx \frac{\epsilon^{4/3}}{n^{1/3}} \left( \frac{\xi}{r_0} \right)^{4/3} \left( \frac{\xi}{\xi(0)} \right)^{2/3}, \quad (\text{A6})$$

$$\frac{\epsilon\xi}{L_c} \approx \left( \frac{nr_0^3}{\epsilon} \right)^{1/3} \left( \frac{r_0\xi^2(0)}{\xi^3} \right)^{1/3}, \quad (\text{A7})$$

$$\tilde{T}_{dp}^s \approx \epsilon^{2/3} \varepsilon_0 (nr_0^3)^{1/3} (r_0\xi^2(0))^{1/3}. \quad (\text{A8})$$

Strictly speaking, formulas (A5)-(A8) are valid if  $\pi r_0^2 \xi(0) n < 1$ . This type of pinning is sometimes called  $\delta l$  pinning.<sup>27</sup> Note that equations (A5)-(A8) and (A1)-(A4) have the same dependences on  $n$ ,  $\epsilon$  and temperature. They thus describe *two different contributions* to one pinning mechanism, with the contribution of Eqs. (A5)-(A8) always dominating when  $r_0 < \xi(0)$ .

If the pinning centers in  $\text{YBa}_2\text{Cu}_3\text{O}_{7-\delta}$  are clusters of oxygen vacancies, it is useful to keep in mind that

$$\frac{4\pi}{3} r_0^3 n = c\delta, \quad (\text{A9})$$

where the constant  $c$  equals 2 if these clusters are formed by  $\text{YBa}_2\text{Cu}_3\text{O}_{6.5}$  phase. Thus, when  $r_0$  decreases at a fixed  $\delta$ , the parameters  $\epsilon\xi/L_c$  and  $\tilde{T}_{dp}^s$  also decrease.

In high- $T_c$  superconductors the pinning can be due to spatial fluctuations in the density of the oxygen vacancies, which results in variations of  $T_c$  over the sample. One has the following estimates for this  $\delta T_c$  pinning:<sup>27</sup>

$$\frac{\epsilon\xi}{L_c} \propto \left( \frac{n\xi}{\epsilon} \right)^{1/3}, \quad (\text{A10})$$

$$\tilde{T}_{dp}^s \propto \epsilon^{2/3} \varepsilon_0 (n\xi^4)^{1/3}, \quad (\text{A11})$$

where  $n$  is the density of oxygen vacancies. This pinning can occur when  $n\xi\xi(0)^3 > 1$ .

The above equations enable us to estimate the temperature dependence of the quantities  $\epsilon\xi/L_c$  and  $\tilde{T}_{dp}^s$ . For this purpose, we insert the expressions

$$\frac{\xi(T)}{\xi(0)} = \frac{\lambda(T)}{\lambda(0)} = \left( 1 - \frac{T^2}{T_c^2} \right)^{-1/2} \quad (\text{A12})$$

in the appropriate formulas. In particular, it follows from Eqs. (10), (A3), (A7) that for  $\delta l$  pinning

$$g_0(t) \equiv \frac{1}{D} \left( \frac{\epsilon\xi(T)}{L_c(T)} \right) = (1 - t^2)^{1/2}, \quad (\text{A13})$$

where  $t \equiv T/T_c$ ,  $D \equiv \epsilon\xi(0)/L_c(0)$ , while according to Eq. (A10), one finds for  $\delta T_c$  pinning

$$g_0(t) = (1 - t^2)^{-1/6}. \quad (\text{A14})$$

- <sup>1</sup> R. Wördenweber, P.H. Kes, and C.C. Tsuei, Phys. Rev. B **33**, 3172 (1986); R. Wördenweber, and P.H. Kes, Cryogenics **29**, 321 (1989).
- <sup>2</sup> S. Bhattacharya and M.J. Higgins, Phys. Rev. Lett. **70**, 2617 (1993); M.J. Higgins and S. Bhattacharya, Physica C **257**, 232 (1996).
- <sup>3</sup> Y. Paltiel, E. Zeldov, Y. Myasoedov, M.L. Rappaport, G. Jung, S. Bhattacharya, M.J. Higgins, Z.L. Xiao, E.Y. Andrei, P.L. Gammel, and D.J. Bishop, Phys. Rev. Lett. **85**, 3712 (2000).
- <sup>4</sup> Y. Paltiel, E. Zeldov, Y.N. Myasoedov, H. Shtrikman, S. Bhattacharya, M.J. Higgins, Z.L. Xiao, E.Y. Andrei, P.L. Gammel, and D.J. Bishop, Nature **403**, 398 (2000).
- <sup>5</sup> S.S. Banerjee, A.K. Grover, M.J. Higgins, G.I. Menon, P.K. Mishra, D. Pal, S. Ramakrishnan, T.V. Chandrasekhar Rao, G. Ravikumar, V.C. Sahoo, S. Sarkar, and C.V. Tomy, Physica C **355**, 39 (2001).
- <sup>6</sup> L. Klein, E.R. Yacoby, Y. Yeshurun, A. Erb, G. Müller-Vogt, V. Breit, and H. Wühl, Phys. Rev. B **49**, 4403 (1994).
- <sup>7</sup> A.A. Zhukov, H. Küpfer, H. Claus, H. Wühl, M. Kläser, and G. Müller-Vogt, Phys. Rev. B **52**, R9871 (1995).
- <sup>8</sup> M. Jirsa, L. Pust, D. Dlouhý, and M.R. Koblishka, Phys. Rev. B **55**, 3276 (1997).
- <sup>9</sup> G.K. Perkins, L.F. Cohen, A.A. Zhukov, and A.D. Caplin, Phys. Rev. B **55**, 8110 (1997).
- <sup>10</sup> K. Deligiannis, P.A.J. de Groot, M. Oussena, S. Pinfold, R. Langan, R. Gagnon, and L. Taillefer, Phys. Rev. Lett. **79**, 2121 (1997).
- <sup>11</sup> H. Küpfer, Th. Wolf, C. Lessing, A.A. Zhukov, X. Lançon, R. Meier-Hirmer, W. Schauer, and H. Wühl, Phys. Rev. B **58**, 2886 (1998).
- <sup>12</sup> T. Nishizaki, T. Naito, and N. Kobayashi, Phys. Rev. B **58**, 11169 (1998).
- <sup>13</sup> S. Kokkaliaris, P.A.J. de Groot, S.N. Gordeev, A.A. Zhukov, R. Gagnon, L. Taillefer, Phys. Rev. Lett. **82**, 5116 (1999); S. Kokkaliaris, A.A. Zhukov, P.A.J. de Groot, R. Gagnon, L. Taillefer, and T. Wolf, Phys. Rev. B **61**, 3655 (2000).
- <sup>14</sup> D. Giller, A. Shaulov, Y. Yeshurun, and J. Giapintzakis, Phys. Rev. B **60**, 106 (1999).
- <sup>15</sup> T. Nishizaki, T. Naito, S. Okayasu, A. Iwase, and N. Kobayashi, Phys. Rev. B **61**, 3649 (2000).
- <sup>16</sup> H. Küpfer, Th. Wolf, R. Meier-Hirmer, and A.A. Zhukov, Physica C **332**, 80 (2000).
- <sup>17</sup> H. Safar, P.L. Gammel, D.A. Huse, D.J. Bishop, W.C. Lee, J. Giapintzakis, and D.M. Ginsberg, Phys. Rev. Lett. **70**, 3800 (1993); G.W. Crabtree, W.K. Kwok, L.M. Paulius, A.M. Petrean, R.J. Olsson, G. Karapetrov, V. Tobos, and W.G. Moulton, Physica C **332**, 71 (2000).
- <sup>18</sup> A. Erb, J.-Y. Genoud, F. Marti, M. Däumling, E. Walker, and R. Flükiger, J. Low Temp. Phys. **105**, 1033 (1996).
- <sup>19</sup> M.B. Gaifullin, Y. Matsuda, N. Chikumoto, J. Shimoyama, and K. Kishio, Phys. Rev. Lett. **84**, 2945 (2000).
- <sup>20</sup> C.J. van der Beek, S. Colson, M.V. Indenbom, and M. Konczykowski, Phys. Rev. Lett. **84**, 4196 (2000).
- <sup>21</sup> M. Avraham, B. Khaykovich, Y. Myasoedov, M. Rappaport, H. Shtrickman, D.E. Feldman, T. Tamegai, P.H. Kes, M. Li, M. Konczykowski, Kees van der Beek, and E. Zeldov, Nature **411**, 451 (2001).
- <sup>22</sup> J. Kierfeld and V. Vinokur, Phys. Rev. B **61**, 14928 (2000).

- <sup>23</sup> T. Giamarchi and P. Le Doussal, Phys. Rev. B **52**, 1242 (1995).
- <sup>24</sup> D. Ertaş and D.R. Nelson, Physica C **272**, 79 (1996).
- <sup>25</sup> T. Giamarchi and P. Le Doussal, Phys. Rev. B **55**, 6577 (1997).
- <sup>26</sup> V. Vinokur, B. Khaykovich, E. Zeldov, M. Konczykowski, and R.A. Doyle, P.H. Kes, Physica C **295**, 209 (1998).
- <sup>27</sup> G. Blatter, M.V. Feigel'man, V.B. Geshkenbein, A.I. Larkin, and V.M. Vinokur, Rev. Mod. Phys. **66**, 1125 (1994).
- <sup>28</sup> E.H. Brandt, Rep. Prog. Phys. **58**, 1465 (1995).
- <sup>29</sup> J. Kierfeld, T. Nattermann, and T. Hwa, Phys. Rev. B **55**, 626 (1997).
- <sup>30</sup> J. Kierfeld, Physica C **300**, 171 (1998).
- <sup>31</sup> M.V. Feigel'man and V.M. Vinokur, Phys. Rev. B **41**, 8986 (1990).
- <sup>32</sup> A.I. Larkin and Yu. N. Ovchinnikov, J. Low Temp. Phys. **34**, 409 (1979).
- <sup>33</sup> E.H. Brandt, J. Low Temp. Phys. **64**, 375 (1986).
- <sup>34</sup> E.H. Brandt, J. Low Temp. Phys. **26**, 709, 735 (1997); *ibid* **28**, 263, 291 (1977).
- <sup>35</sup> The correlation functions  $u(R, 0)$  in the Bragg glass and in the amorphous vortex glass are *qualitatively* different<sup>23</sup> at  $R > R_a$ . Therefore, these vortex solid phases cannot be *continuously* transformed into each other, and a termination of the phase transition line separating these phases cannot occur below the melting line. This phase transition line can terminate only on another phase transition line (i.e., on the melting curve).
- <sup>36</sup> The upper region of single vortex pinning was discussed by Larkin and Ovchinnikov<sup>32</sup> in the context of the origin of the peak effect in low- $T_c$  superconductors. Without account of thermal fluctuations, this region exists at magnetic fields near  $H_{c2}(t)$  (when  $1 - h_{sv}(t) \leq h \leq 1$ ). This follows from Eq. (8), which gives  $u^2(a, 0) = \xi^2$  at  $h = 1 - h_{sv}$ . Note that we show the boundary of this region only in Fig. 5.
- <sup>37</sup> G.P. Mikitik, Physica C **245**, 287 (1995).
- <sup>38</sup> A. Houghton, R.A. Pelcovits, and A. Sudbo, Phys. Rev. B **40**, 6763 (1989).
- <sup>39</sup> E.H. Brandt, Phys. Rev. Lett. **63**, 1106 (1989).
- <sup>40</sup> I.M. Babich, Yu.V. Sharlai, and G.P. Mikitik, Fiz. Nizk. Temp. **20**, 227 (1994) [Low Temp. Phys. **20**, 220 (1994)].
- <sup>41</sup> Note that the depinning line presented in Fig. 4 has a descending (with  $t$ ) branch which is not shown in Fig. 18 of Ref. 27. This branch is due to the factor  $(1 - h)^{-3/2}$  in Eq. (17), which was neglected in Eq. (4.88) of Ref. 27. (Of course, the part of the depinning line lying above the melting curve has only formal meaning, since we did not take into account that the shear modulus  $c_{66}$  vanishes at the melting.)
- <sup>42</sup> P.A. Lee and S.R. Shenoy, Phys. Rev. Lett. **28**, 1025 (1972).
- <sup>43</sup> G.P. Mikitik, Zh. Eksp. Teor. Fiz. **101**, 1042 (1992) [Sov. Phys. JETP **74**, 558 (1992)].
- <sup>44</sup> W.K. Kwok, J.A. Fendrich, C.J. van der Beek, and G.W. Crabtree, Phys. Rev. Lett. **73**, 2614 (1994).
- <sup>45</sup> J. Shi, X.S. Ling, R. Liang, D.A. Bonn, and W.N. Hardy, Phys. Rev. B **60**, R12593 (1999).
- <sup>46</sup> X.S. Ling, S.R. Park, B.A. McClain, S.M. Choi, D.C. Dender, and J.W. Lynn, Phys. Rev. Lett. **86**, 712 (2001).
- <sup>47</sup> A.I. Larkin, M.C. Marchetti, and V.M. Vinokur, Phys. Rev. Lett. **75**, 2992 (1995).
- <sup>48</sup> C. Tang, X. Ling, S. Bhattacharya, and P.M. Chaikin, Europhys. Lett. **35**, 597 (1996).
- <sup>49</sup> J.A. Fendrich, W.K. Kwok, J. Giapintzakis, C.J. van der Beek, V.M. Vinokur, S. Fleshler, U. Welp, H.K. Viswanathan, and G.W. Crabtree, Phys. Rev. Lett. **74**, 1210 (1995).
- <sup>50</sup> D. Lopez, L. Krusin-Elbaum, H. Safar, E. Righi, F. de la Cruz, S. Grigera, C. Feild, W.K. Kwok, L. Paulius, and G.W. Crabtree, Phys. Rev. Lett. **80**, 1070 (1998).
- <sup>51</sup> Y. Nonomura and Xiao Hu, Phys. Rev. Lett. **86**, 5140 (2001).
- <sup>52</sup> E.V. Thuneberg, J. Kurkijärvi, and D. Rainer, Phys. Rev. Lett. **48**, 1853 (1982).
- <sup>53</sup> A.M. Campbell and J.E. Evetts, Adv. Phys. **21**, 199 (1972).

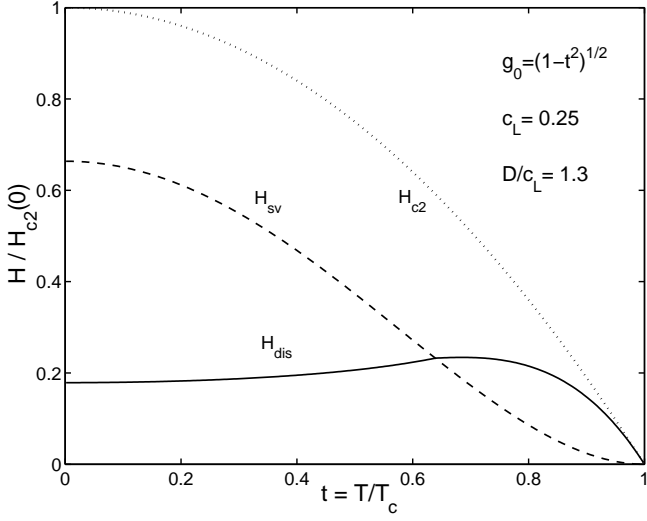


FIG. 1. The order-disorder line  $H_{dis}(t)$  (solid line) calculated from Eqs. (4), (9), (A13) ( $\delta l$  pinning) for  $c_L = 0.25$  and  $D/c_L = 1.3$ . Simplified approach, without account of thermal fluctuations. The boundary of the single vortex pinning regime,  $H_{sv}(t)$ , is given by the dashed line, and the dotted line shows the mean-field upper critical field  $H_{c2}(t) = H_{c2}(0)(1 - t^2)$ .

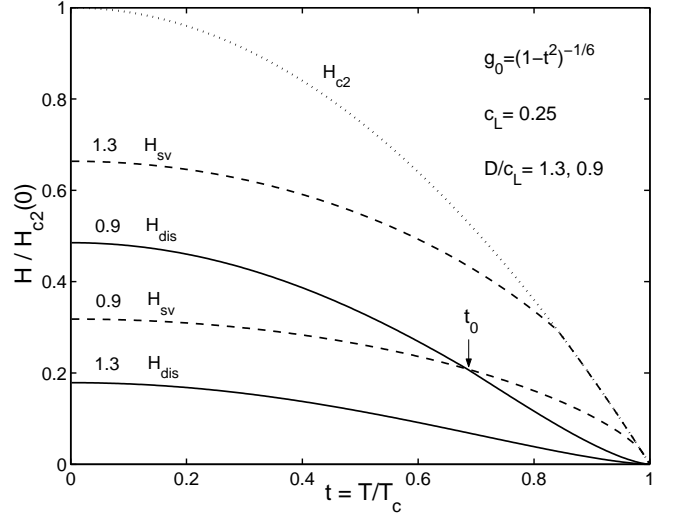


FIG. 3. The lines  $H_{dis}(t)$  and  $H_{sv}(t)$  as in Figs. 1, 2 but for  $\delta T_c$  pinning, Eq. (A14), for  $D/c_L = 1.3$  and  $0.9$ . Now  $H_{dis}(t)$  and  $H_{sv}(t)$  cross at  $t = t_0$  for  $D/c_L < 1$ .

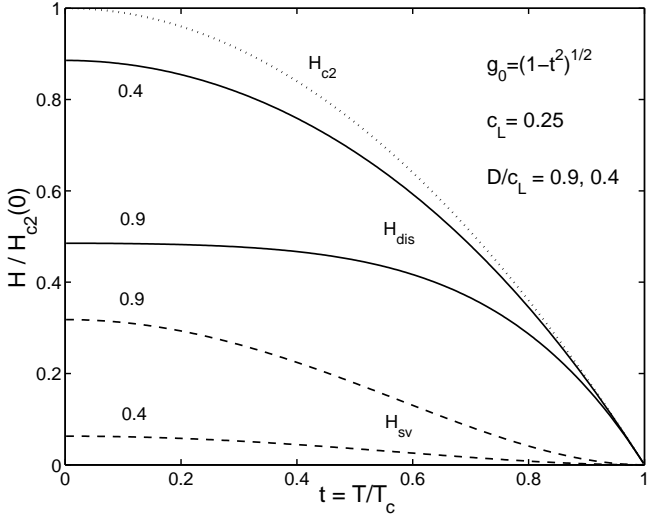


FIG. 2. As Fig. 1 but for  $D/c_L = 0.9$  and  $0.4$ . Note that for  $D/c_L < 1$  the order-disorder line  $H_{dis}(t)$  does not intersect the single vortex pinning boundary  $H_{sv}(t)$ .

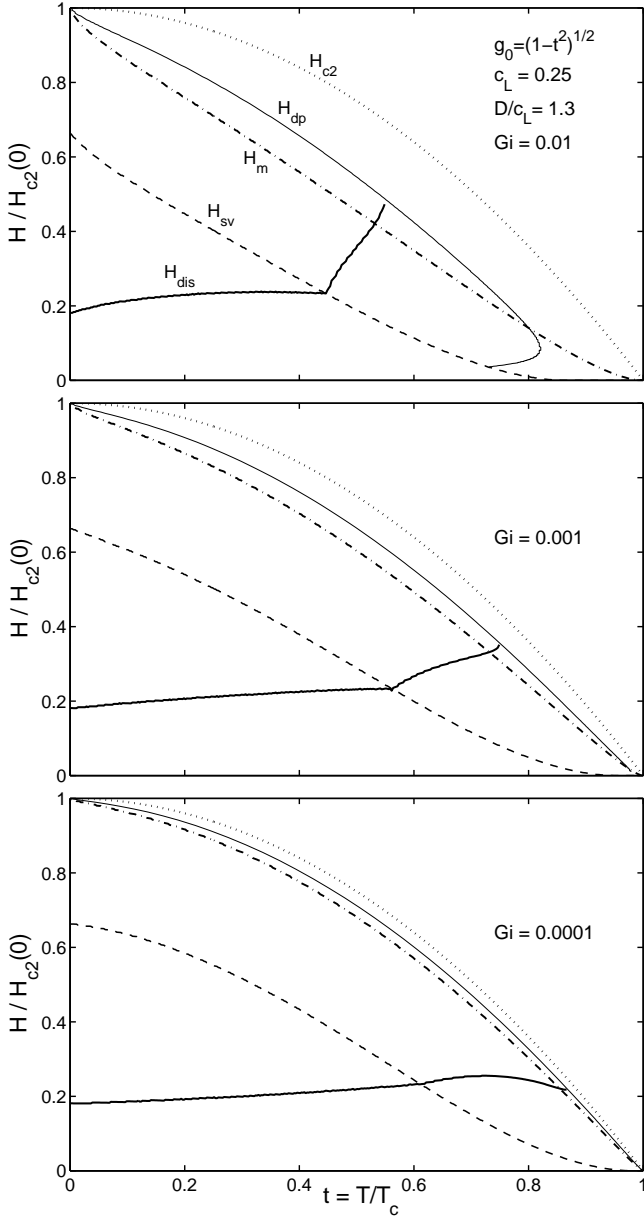


FIG. 4. The order-disorder line  $H_{dis}(t)$  (bold solid line) calculated from Eqs. (22), (24), (A13) ( $\delta l$  pinning), which account for thermal fluctuations, for  $c_L = 0.25$ ,  $D/c_L = 1.3$ , and for three values of the Ginzburg number  $Gi = 0.01$ ,  $0.001$ , and  $0.0001$  (from top to bottom). Also shown are the boundary of the single vortex pinning regime  $H_{sv}(t)$ , Eq. (19) (dashed line), the mean-field  $H_{c2}(t) = H_{c2}(0)(1 - t^2)$  (dotted line), the vortex-lattice melting line  $H_m(t)$ , Eq. (25) (dashed-dotted line), and the depinning line  $H_{dp}(t)$ , Eqs. (16)-(18) (thin solid line), along which one formally has  $u_T^2 = \xi^2$  and where  $H_{dis}(t)$  ends. The short part of  $H_{dis}$  above  $H_m$  has no physical meaning.

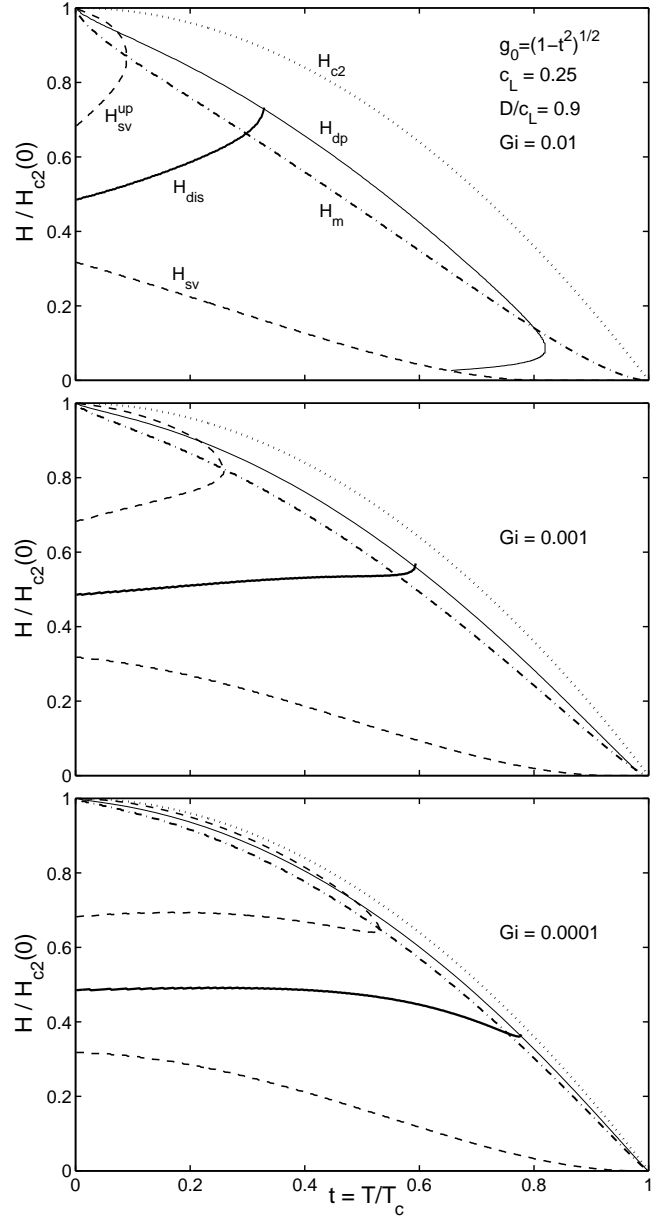


FIG. 5. As Fig. 4 but for different  $D/c_L = 0.9$ . The dashed lines show the boundaries of both the lower ( $H_{sv}$ ) and upper ( $H_{sv}^{up}$ ) regions of single vortex pinning, see Eq. (21) and text.

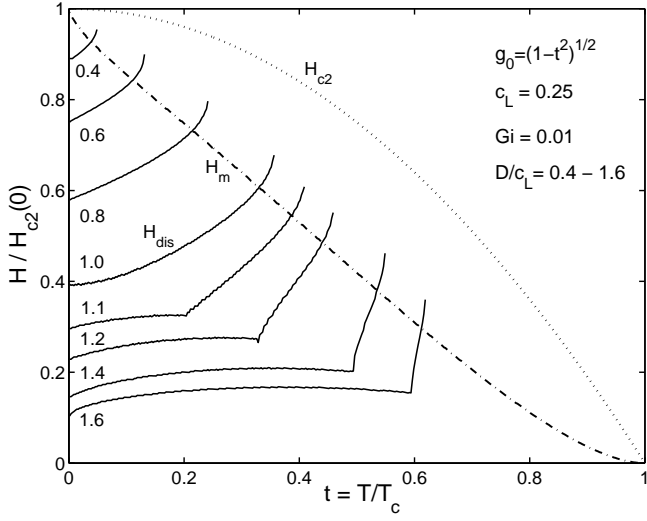


FIG. 6. The order-disorder lines  $H_{dis}(t)$  (bold solid lines) according to Eqs. (22), (24), (A13) ( $\delta l$  pinning) for  $c_L = 0.25$ ,  $Gi = 0.01$  and several values  $D/c_L = 0.4$  to  $1.6$ . The dash-dotted line is the vortex-lattice melting line  $H_m(t)$ , Eq. (25), and the dotted line indicates  $H_{c2}(t) = H_{c2}(0)(1-t^2)$ .

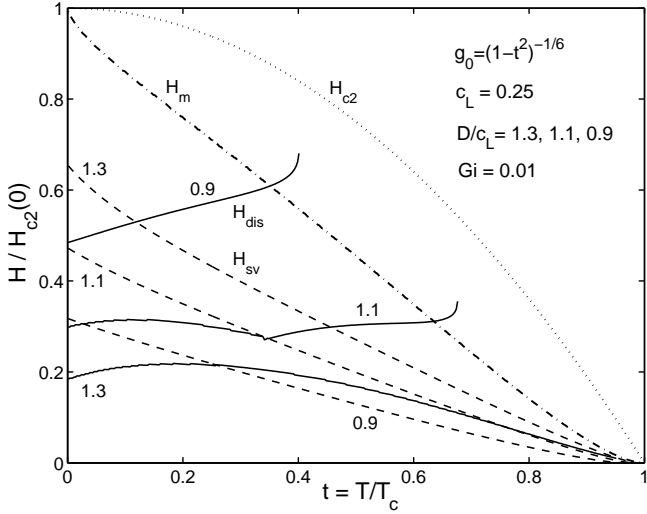


FIG. 7. The order-disorder lines  $H_{dis}(t)$  (solid lines) as in Fig. 6 but for  $\delta T_c$  pinning, (A14), for  $D/c_L = 1.3$ ,  $1.1$ , and  $0.9$ . The dashed lines are the single-vortex pinning boundaries  $H_{sv}(t)$ , Eq. (19), the dash-dotted line is the melting line  $H_m(t)$ , Eq. (25), and the dotted line indicates  $H_{c2}(t) = H_{c2}(0)(1-t^2)$ .

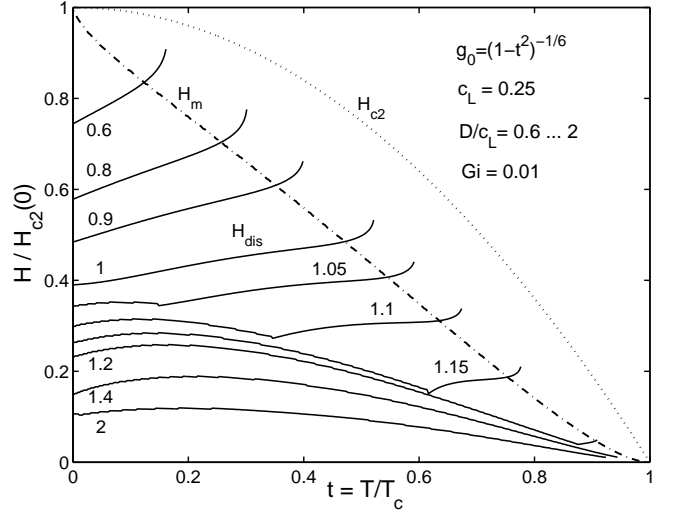


FIG. 8. The order-disorder lines  $H_{dis}(t)$  (solid lines) as in Fig. (7) with (A14), but for many values  $D/c_L = 0.6$  to  $2$ .

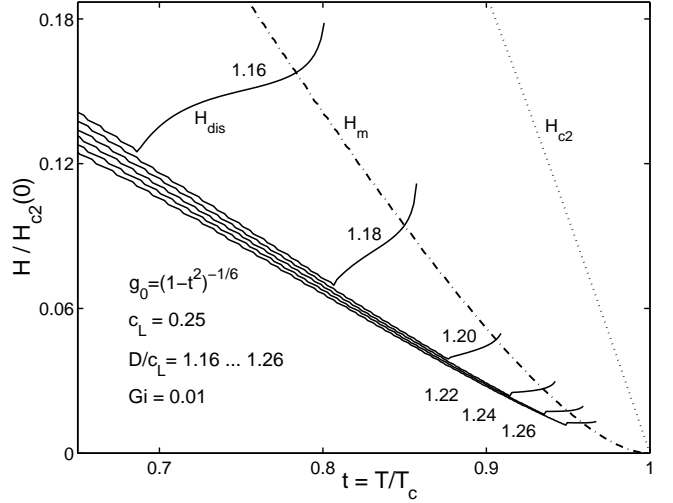


FIG. 9. As Fig. 8 but enlarged scale, for  $D/c_L = 1.16$  to  $1.26$ . This figure simulates the evolution of the  $H-T$  phase diagram for  $\text{YBa}_2\text{Cu}_3\text{O}_{7-\delta}$  crystals when the oxygen deficiency  $\delta$  is changed.

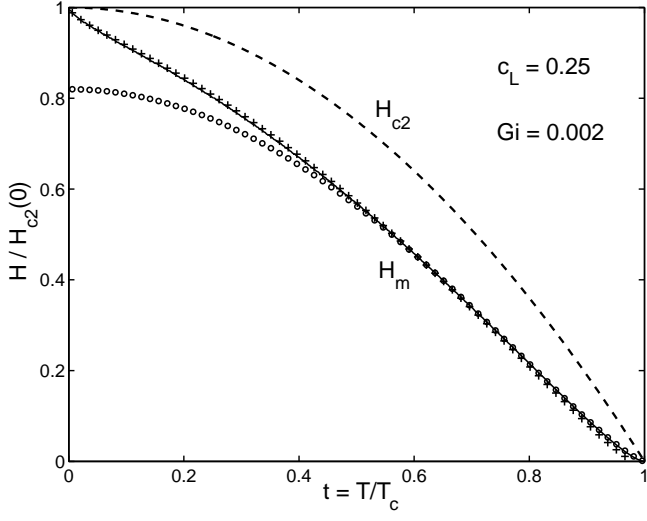


FIG. 10. The vortex-lattice melting-line  $H_m(t)$  from Eq. (25) (solid line) and its approximations Eq. (26) (crosses) and Eq. (28) (circles) with  $A = 0.82$  and  $\gamma = 1.31$ . The dashed line indicates  $H_{c2}(t) \propto 1 - t^2$ . Here  $c_L = 0.25$  and  $Gi = 0.002$ .

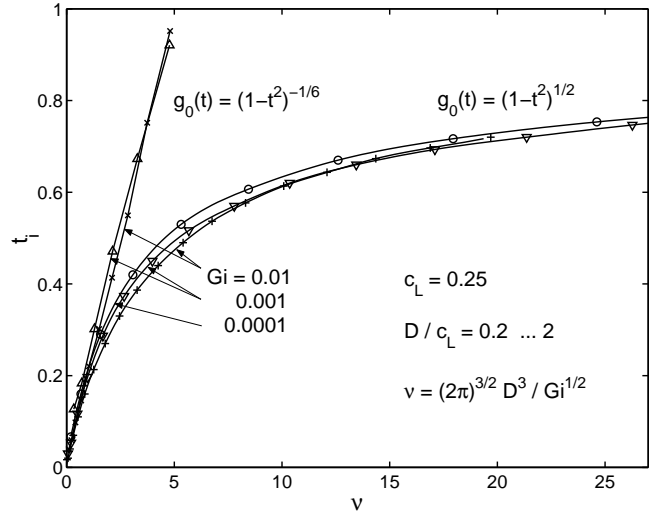


FIG. 11. The temperature  $t_i$  where the melting line and the order-disorder line cross, plotted versus the parameter  $\nu = (2\pi)^{3/2} D^3 / Gi^{1/2}$ . This temperature is found by calculating the phase diagrams from Eqs. (19)-(25) with  $c_L = 0.25$  and Eq. (A13) (right 3 curves) or Eq. (A14) (left 2 curves) for  $Gi = 0.01$  (crosses),  $Gi = 0.001$  (triangles), and  $Gi = 0.0001$  (circles). The interval of  $D/c_L$  actually used for each curve can be calculated from  $Gi$  and the  $\nu$  interval.